

Fig. 4. Hugoniot data of stishovite and calculated Hugoniot and 300°K isotherm from case 3 (Table 4). Symbols are those used in Figure 1.

The last two cases were rerun with  $K_0$  given the fixed value of 3.45 Mb, which gives an isentropic bulk modulus very close to that given by Mizutani *et al.* [1972]. (In all cases given here, the isentropic bulk modulus is about 0.02 Mb greater than the isothermal bulk modulus.) The results are given in Table 4 (cases 4 and 5). The changes from the previous solutions are small. The standard errors are calculated with the 0.24-Mb error given by Mizutani *et al.* for the bulk modulus.

In view of the current discussion of the relative merits of the Lagrangian and Eulerian formulations of finite strain [Thomson, 1970, 1972; G. F. Davies, unpublished manuscripts, 1972], the dependence of the preceding results on the form of the equation of state should be tested. This testing was done by using a Lagrangian isotherm [Thomson, 1970; G. F. Davies, unpublished manuscript, 1972] but keeping (5) for  $\gamma$ . This formulation does not correspond to the Lagrangian equation used by Thomson [1970], who used a different expression for  $\gamma$ . This formulation has been discussed previously (G. F. Davies, unpublished manuscript, 1972). In any case, using a different equation for  $\gamma$  should yield a significantly different value for  $(\partial K/\partial T)_P$  only, for which we have no other control. Cases 2 and 3 were repeated with the Lagrangian iso-

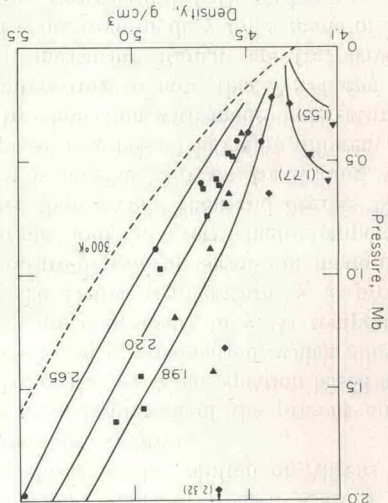


Fig. 2. Hugoniot data of stishovite and calculated Hugoniot and 300°K isotherms from case 1 (Table 4). Symbols are those used in Figure 1.

are systematically low because the anvils of the tetrahedral press used by Bassett and Barnett may have come into contact at about this pressure. These points were not used in the present analysis. The calculated isotherms agree with the remaining data within the scatter of the data.

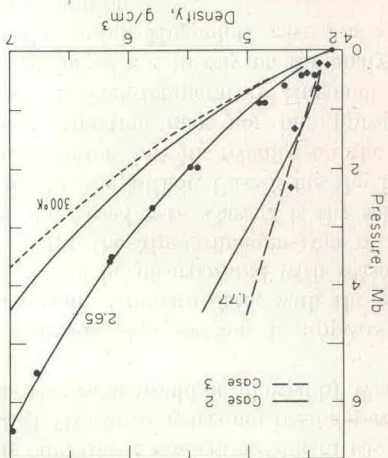


Fig. 3. Very high-pressure Hugoniot data of stishovite and calculated Hugoniot and isotherms from case 2 (solid line) and case 3 (dashed line). Only the Hugoniot corresponding to initial densities 2.65 and 1.77 g/cm<sup>3</sup> are shown. Symbols are those used in Figure 1.

therm. The results are given in Table 4 (cases 2a and 3a). The values of  $K_0$  are comparable, those of  $K_0'$  somewhat lower, those of  $K_0 K_0''$  much higher, and those of the other parameters comparable to the corresponding values in cases 2 and 3. In particular, the value of  $\alpha$  is very little changed; it is still much lower than the value given by Weaver [1971].

Ahrens *et al.* [1970] interpreted the  $\rho_0' = 1.98 \text{ g/cm}^3$  data as indicating a reversal in the slope of the Hugoniot at about 1.2 Mb (Figure 1). A criterion was given relating the density at which the slope of the Hugoniot becomes infinite to the value of  $\gamma$  at that point:  $\gamma = 2/[(\rho/\rho_0') - 1]$ . However, it can be seen from equation 12 for the Hugoniot that the Hugoniot pressure also becomes infinite at this density; in other words, the Hugoniot pressure asymptotes to infinity rather than 'bends over.' This interpretation biased the high-pressure values of  $\gamma$  to lower values, since it favored an interpretation in which the Hugoniot were crowded together at these compressions. The discrepancy between the results of Ahrens *et al.* [1970] and those of this study is due partly to the last effect, partly to the fewer data available at the time, and partly

to the higher value of  $\alpha$  used. Case 1 given here is closer to the solution of Ahrens *et al.* and shows similar effects.

The main limitation of the present analysis is probably the use of an equation based on the Mie-Grüneisen approximation, which allows no temperature dependence of  $\gamma$ . At temperatures below the Debye temperature,  $\gamma$  is probably temperature-dependent because of mode undersaturation, and, at very high temperatures (greater than several thousand degrees Kelvin, say), it is possible that we are dealing with a fluid phase (see below) having a different value of  $\gamma$ . In connection with mode undersaturation, it is interesting to note that Nicol and Fong [1971], measuring Raman spectra, have observed a negative mode  $\gamma$  for a mode of rutile, which is isostructural with stishovite.

The temperature dependence of  $\alpha$  is dominated by the temperature dependence of  $C_p$  and possibly of  $\gamma$  (see equation 2). Weaver [1971] notes that his value of  $\epsilon = (\partial\alpha/\partial T)_p/\alpha^2 = 33 \pm 17$  seems too small; it implies that  $(\partial\gamma/\partial T)_p = -5 \times 10^{-3}/^\circ\text{K}$ , a value sufficient to reduce  $\gamma$  to zero within  $300^\circ\text{K}$ . With  $(\partial\gamma/\partial T)_p = 0$ , Weaver estimates that  $\epsilon = 190 \pm 20$ . If we take Weaver's mean value of  $\alpha$  in the range  $300^\circ\text{--}900^\circ\text{K}$  (i.e.,  $\alpha = 18.6 \times 10^{-6}/^\circ\text{K}$ ) to apply to  $600^\circ\text{K}$  and combine it with the  $300^\circ\text{K}$  value of  $13 \times 10^{-6}/^\circ\text{K}$  found here, we get  $\epsilon = 100$  approximately. This value is intermediate, and thus a moderate value of  $(\partial\gamma/\partial T)_p$  is implied. Of course, it has not been determined whether this value would be allowed by Weaver's data.

To conclude this section, it appears that most relevant stishovite data, with the exception of  $\alpha$ , can be incorporated with reasonable accuracy into the Mie-Grüneisen-type of equation of state used here. Case 2 is the solution preferred by the author. Case 3 fits the Hugoniot data better, but its reliance on the Mie-Grüneisen equation may not be appropriate for the very high-temperature Hugoniot data. If it is preferred not to rely on the analysis of any of the porous Hugoniot, case 1 is an appropriate solution.

'*Coesite.*' This section will assume that the Hugoniot of the most porous quartz samples represent coesite. The difficulties raised by this assumption and an alternative interpretation will be discussed in the next section.

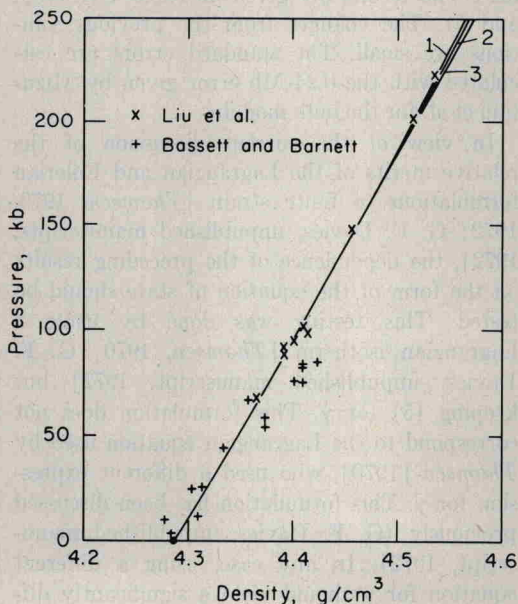


Fig. 5. Static-compression data of stishovite compared with  $300^\circ\text{K}$  isotherms calculated from cases 1, 2, and 3.